Collisionless shock resolution in nematic liquid crystals

Gaetano Assanto,[1,*] T. R. Marchant,[2,†] and Noel F. Smyth[3,‡]
[1]*NooEL—Nonlinear Optics and OptoElectronics Laboratory, Department of Electronic Engineering, INFN-CNISM-University "'Roma Tre,'" Via della Vasca Navale 84, 00146 Rome, Italy*
[2]*School of Mathematics and Applied Statistics, The University of Wollongong, Wollongong 2522, N.S.W., Australia*
[3]*School of Mathematics and the Maxwell Institute for Mathematical Sciences, University of Edinburgh, The King's Buildings, Mayfield Road, Edinburgh, Scotland EH9 3JZ, United Kingdom*
(Received 10 October 2008; published 3 December 2008)

The diffractive resolution on a collisionless shock formed along the spatial profile of a beam in a nematic liquid crystal is considered, this material being an example of a self-focusing, nonlocal medium. It is found that the shock is resolved through the formation of an undular bore structure which persists for experimentally relevant propagation distances due to nonlocality delaying the onset of modulational instability. Both 1+1 and 2+1 dimensional bores with circular symmetry are considered (termed line and circular bores, respectively). A semianalytical solution is developed for the line undular bore, approximating it as a train of uniform solitary waves. The predictions of this semianalytical theory are found to be in excellent agreement with numerical solutions of the governing equations, both for line and circular bores. The method presented here yields semianalytical results for a bore in focusing media.

DOI: 10.1103/PhysRevA.78.063808 PACS number(s): 42.65.Tg, 42.70.Df

I. INTRODUCTION

Spatial solitary waves in bulk media result from a balance between the diffractive spreading of a light beam and nonlinear, nonlocal self-focusing. Such solitary waves have generated much interest due to their possible applications as reconfigurable "circuits" for all-optical information processing [1]. One particular nonlinear, nonlocal optical medium which has received much attention is a nematic liquid crystal, due in part to its "huge" nonlinear response which allows nonlinear effects to be observed at small excitations [2]. A series of elegant experiments have shown that stable spatial solitary waves, so-called nematicons, can propagate in nematic liquid crystals at mW powers and over ~mm distances [3–5].

The equations governing nematicon propagation in liquid crystals (termed the nematicon equations) are a coupled system of two nonlinear partial differential equations in 2+1 dimensions and, as such, are difficult to solve, with no known exact solutions. For this reason most existing work has been numerical [4,6] or based on a mix of various asymptotic, approximate, and numerical methods [7–10].

Previous work carried out in the frame of nematic liquid crystals considered the development of modulational instability (MI) for continuous wave solutions of the nematic equations [11–14]. Experimental results demonstrate that an initial wide input beam develops a periodic pattern as the propagation distance increases, which is progressively amplified. Analysis of the fast Fourier transform (FFT) spectrum of the intensity shows that the maximum gain is in good agreement with the predictions of a stability analysis. References [15,16] also investigated MI for anisotropic nematics in the presence of birefringent walkoff.

A generalized focusing nonlinear Schrödinger (NLS) equation with three additional terms representing third-order dispersion, self-steepening, and intrapulse stimulated Raman scattering (SRS) was studied in [17]. They found an analytical kink solution of this equation which resolves an optical shock in a smooth, monotonic manner with no oscillation. This kink solution is a viscous bore, with the SRS giving the required loss, as opposed to the lossless, nonstationary, oscillatory bores examined in the present work. They further considered the numerical evolution of pulses consisting of kink-antikink pairs and a super-Gaussian profile and found that there is a redshift in the pulse spectra, which is typical of SRS. Reference [18] also considered an NLS equation with an SRS term and found a kink (viscous bore) solution which generalized that of Agrawal and Headley [17]. This kink solution could be either monotone or oscillatory, depending on the parameter choices. Last, the kink was found to be unstable in both the focusing and defocusing regimes.

Reference [19] addressed the development of MI in a medium governed by a nonlocal, nonlinear Schrödinger equation. A stability analysis showed that MI always occurs for the focusing case, while in the defocusing case the occurrence of MI is dependent on the particular form of the response function. Gaussian, which corresponds to the nematicon equations in 1+1 dimensions, and rectangular response functions were considered in detail. The MI gain profiles showed that the maximum gain decreases as the degree of nonlocality increases, which confirms that nonlocality can suppress the development of modulation instability, but cannot eliminate it. A modulational transverse stability analysis of long, one dimensional beams for the (focusing) nematicon equations was undertaken by Lin *et al.* [20] and, again, nonlocality was found to suppress modulational instability. While these works considered axisymmetric beams, Conti *et al.* [16] considered MI for anisotropic nematics.

More recently Ref. [21] addressed the development of collisionless shock waves in nonlocal media, both focusing and defocusing. In the focusing case it was shown that non-

*assanto@uniroma3.it
†tim_marchant@uow.edu.au
‡N.Smyth@ed.ac.uk

locality suppresses modulational instability, so that the development of an undular bore from the shock could be seen. The defocusing case is modulationally stable, so that the shock develops into a stable undular bore consisting of dark nematicons. Experimental results were presented in Ghofraniha *et al.* [21] for the development of a shock in a thermal (defocusing) medium, with good qualitative comparisons obtained with numerical results. A similar study of collisionless shock and bore formation in a defocusing photorefractive crystal was reported in Wan *et al.* [22]. Nematic liquid crystals form ideal media for such studies as they exhibit a self-focusing response to electrical fields and a defocusing thermal response [2].

For nonlinear dispersive (or diffractive) wave equations, initial discontinuities are resolved through dispersion (diffraction) into an undular bore, which is a modulated wave train consisting of solitary waves at its leading edge and linear waves at its trailing edge. An undular bore then gives a smooth transition across the discontinuity. Mathematically, undular bore solutions are derived using Whitham modulation theory [23]. Modulation theory develops partial differential equations for the parameters of a slowly varying wave train. In general, if these modulation equations are hyperbolic, the wave train is modulationally stable and the undular bore solution is found as a simple wave solution. If the modulation equations are elliptic, the wave train is modulationally unstable and there is no long-term undular bore solution. In a study of the forced Korteweg–de Vries (KdV) equation for resonant fluid flow over topography, Grimshaw and Smyth [24] and Smyth [25] used the undular bore solution of the KdV equation to describe this resonant flow. As part of their study, Grimshaw and Smyth [24] approximated the undular bore by a train of uniform solitons and found good agreement with numerical solutions for a wide range of parameter values. The method, termed uniform soliton theory, has also been applied to the modified KdV initial-boundary value (IBV) problem [26] and an IBV problem for magma flow [27], with good agreement between numerical and theoretical results.

In this paper we consider the evolution of a collisionless shock for the nematicon equations. Continuous waves for the focusing nonlinear Schrödinger (NLS) type nematicon equations are unstable, have elliptic modulation equations and so a shock boundary condition is ill posed. However, it is shown that the propagation distance for the development of MI is longer than that for a bore and longer than the propagation distance in experimental scenarios, depending on the noise level. In Sec. II the governing equations are presented, along with a stability analysis for a continuous wave in 1 +1 dimensions. In Sec. III the semianalytical solution for the undular bore evolving from a shock is developed for the 1 +1 dimensional line bore geometry. This semianalytical solution is based on a train of nematicons. As there is no exact solution for a steady nematicon, a variational method is adopted to obtain an approximation to it. Mass, momentum, and energy conservation are then used to obtain approximate solutions for the amplitude, spacing and velocity of the nematicons being generated by the bore. In Sec. IV the semianalytical solutions are compared with numerical results for line and circular bores, with excellent agreement found. Numerical simulations are also performed to investigate the onset of MI for an undular bore. In Sec. V the results are summarized.

II. GOVERNING EQUATIONS

Let us consider coherent, polarized light propagating in a liquid crystal cell, with the Z coordinate down the axis of the cell and the (X,Y) coordinates orthogonal to this direction. Let us take the input light to be polarized in the X direction. To overcome the Freéderick threshold a static electric field is applied in the X direction so that in the absence of light the nematic director (i.e., the optic axis distribution of the corresponding uniaxial crystal) makes an angle $\hat{\theta}$ to the Z direction in the plane (X,Z), as in [3]. We then set θ to be the perturbation of the director angle from this pretilt angle due to the optical field and E to be the electric field envelope of the light. Due to walkoff the light beam propagates at an angle to the Z direction [28]. Let us take the coordinate z to be in the walkoff direction, with x and y orthogonal to this. In nondimensional variables the equations governing the propagation of light through the liquid crystal cell are then

$$i\frac{\partial E}{\partial z} + \frac{1}{2}\nabla^2 E + \sin(2\theta)E = 0,$$

$$\nu\nabla^2\theta - q\sin 2\theta = -2|E|^2\cos 2\theta, \tag{1}$$

where the Laplacian ∇^2 is in the (x,y) plane [7,9,30]. However, unless the nematicon paths are curved, due to a changing electric field say, the difference between the x,y,z and X,Y,Z coordinate systems is small and may be neglected. The parameter ν measures the elasticity of the nematic and q is related to the energy (squared amplitude) of the static electric field which pretilts the nematic [5,7,8,30]. The usual operating regime for nonlinear guided wave propagation in nematic liquid crystals is the so-called nonlocal regime in which ν is large [7], with $\nu/q \approx 25$ for optical solitons [29].

So let us consider the nonlocal limit, for which ν is large. In this limit the response of the molecular director to the electric field is nonlocal, due to the slow decay of the crystal distortion produced by the optical field. It can then be seen from the director equation, the second of Eq. (1), that θ is small [7], so the nematicon equations (1) can be approximated by

$$i\frac{\partial E}{\partial z} + \frac{1}{2}\nabla^2 E + 2\theta E = 0, \quad \nu\nabla^2\theta - 2q\theta = -2|E|^2. \tag{2}$$

A. Boundary conditions for the line bore

Before considering the general 2+1 dimensional case, let us consider the case in which the breaking front is a one dimensional plane. In the present work we are interested in the subsequent diffractive smoothing of the shock formed in a nonlocal, self-focusing medium as considered in [21]. Therefore let us assume that the shock has formed, so that the appropriate boundary condition in 1+1 dimensions is

$$E = \begin{cases} a_m e^{i(kx-\omega z)}, & x<0, \\ 0, & x>0, \end{cases} \qquad \theta = \begin{cases} \dfrac{a_m^2}{q}, & x<0, \\ 0, & x>0 \end{cases} \tag{3}$$

at $z=0$, where

$$\omega = \frac{k^2}{2} - \frac{2a_m^2}{q}. \tag{4}$$

The wave in the region $x<0$ is the continuous wave (cw) solution of Eq. (2). Without loss of generality we can assume $a_m>0$. Once the smoothing of the shock in 1+1 dimensions has been analyzed and the appropriate solution obtained, this solution will be extended to the experimentally more realistic 2+1 dimensional case.

B. Stability of the 1+1 dimensional continuous wave

It is well known that, for focusing NLS-type equations such as the nematicon equations (2), linear waves are unstable [1]. In terms of Whitham's modulation theory [23], the modulation equations for focusing NLS-type equations are elliptic. As these stability results are well known [11], here we shall just summarize the basic points. Let us consider a cw and perturb the electric field and the optic axis distribution by small quantities as

$$E = a_m e^{i(2a_m^2/q)z}(1-\epsilon), \quad \theta = \frac{a_m^2}{q}(1+\theta_1), \tag{5}$$

where $|\epsilon|, |\theta_1| \ll 1$. Let us then seek a modal expansion for the perturbation of the form

$$\epsilon = Ae^{\lambda z}e^{i\mu x} + Be^{\lambda z}e^{-i\mu x}, \tag{6}$$

which is then substituted into the nematicon equations (2), giving

$$\lambda = \pm \frac{|\mu|}{2}\left[\frac{16a_m^2}{(2q+\nu\mu^2)} - \mu^2\right]^{1/2}. \tag{7}$$

Hence the cw is unstable if

$$0 < \mu^2 < \frac{-q + (q^2 + 16\nu a_m^2)^{1/2}}{\nu}. \tag{8}$$

This stability result is the same, suitably rescaled, as Eq. (39) in [19]. In the local limit $\nu \to 0$ the NLS modulational stability result is retrieved [1,23]. In the highly nonlocal limit, $\nu \to \infty$, the instability band (8) becomes $(0, 8^{1/2}\nu^{-1/2})$ and the maximum rate of instability becomes $\lambda_{max} = (2/\nu)^{1/2}a_m$. It can be clearly seen that as ν increases the modulational instability is suppressed.

III. SEMIANALYTICAL SOLUTIONS

A. The 1+1 dimensional semianalytical nematicon solution

The previous section showed that cw solutions of the nematicon equations (2) are unstable. Hence the modulation equations associated with them are elliptic [23]. The usual method to find undular bores of nonlinear wave equations is to construct the associated modulation equations and, if these equations are hyperbolic, find the undular bore as a simple wave solution [31]. The modulation equations for the nematicon equations (2) are elliptic and so do not possess a simple wave solution. However the results of [21] and the present numerical results show that an undular bore structure forms from a breaking front, or shock wave, for a certain length z, before modulational instability takes over and the bore is destroyed. As the standard method based on modulation theory will not work, an alternative method developed by Grimshaw and Smyth [24] for the KdV equation, and subsequently applied to other equations [27,32,33], will be employed. This method assumes that the shock is smoothed out into a series of equal amplitude solitons. Even though this is not true in the initial stages of the evolution, it becomes a better approximation as z increases as the number of waves in the bore becomes large [24].

The bore approximation of Grimshaw and Smyth [24] is based on the exact soliton solution of the KdV equation. No such exact solution of the nematicon equations (2) exists. Therefore a variational approximation to this soliton solution will be used, which was found to be accurate in previous work on nematicon evolution [8–10]. The variational approximation to the nematicon in 1+1 dimensions will be sought before the approximation to the undular bore is found.

The nematicon equations (2) have the Lagrangian

$$L = i(E^*E_z - EE_z^*) - |\nabla E|^2 + 4\theta|E|^2 - \nu|\nabla\theta|^2 - 2q\theta^2, \tag{9}$$

where the * superscript denotes the complex conjugate. An approximate steady nematicon solution in 1+1 dimensions can be sought using a trial function similar to that used by Minzoni *et al.* [10] in 2+1 dimensions:

$$E = a\,\mathrm{sech}\,\frac{x-kz}{w}e^{i(kx+\sigma z)}, \quad \theta = \alpha\,\mathrm{sech}^2\,\frac{x-kz}{\beta}. \tag{10}$$

The trial function in the electric field is based on the soliton solution of the NLS equation and has profile amplitude a and width w. Note that k is chosen to be the same as the wave number in the cw initial profile. Also, the propagation constant $V=k$ is not an assumption but an exact result deduced from the traveling wave form of the governing equations. The director distribution has optic axis perturbation amplitude α and width β. In the nonlocal limit $\beta \gg w$. These trial functions (10) are now substituted into the Lagrangian (9), which is then averaged by integrating from $-\infty$ to ∞ in x. This results in the averaged Lagrangian

$$\mathcal{L} = -4a^2w\sigma - 2k^2a^2w - \frac{2a^2}{3w} - \frac{16\nu\alpha^2}{15\beta} - \frac{8}{3}q\alpha^2\beta + \alpha a^2 I, \tag{11}$$

where

$$I(w,\beta) = \int_{-\infty}^{\infty} \mathrm{sech}^2\left(\frac{x}{\beta}\right)\mathrm{sech}^2\left(\frac{x}{w}\right)dx. \tag{12}$$

For $\beta \neq w$ the integral I cannot be evaluated in closed form. The variational equations, which provide the nematicon parameters, are then

$$\mathcal{L}_a = -8aw\sigma - 4k^2aw - \frac{4a}{3w} + 2\alpha aI = 0, \tag{13}$$

$$\mathcal{L}_w = -4a^2 - 2k^2a^2 + \frac{2a^2}{3w^2} + \alpha a^2 I_w = 0, \tag{14}$$

$$\mathcal{L}_\alpha = -\frac{32\nu\alpha}{15\beta} - \frac{16}{3}q\alpha\beta + a^2 I = 0, \tag{15}$$

$$\mathcal{L}_\beta = \frac{16\nu\alpha^2}{15\beta^2} - \frac{8}{3}q\alpha^2 + \alpha a^2 I_\beta = 0. \tag{16}$$

From Eqs. (13) and (14) we have

$$\alpha = \frac{4}{3w(I - wI_w)}, \tag{17}$$

which is the amplitude of the optic axis distribution. The variational equations (15)–(17) then represent three equations in the four unknown parameters which describe the director and electric field profiles. These equations were solved numerically for the nematicon parameters, when one of them had a given value as the nematicon solution is a one parameter family. The integral I was evaluated numerically using Simpson's rule. When $\nu=0$ the governing equations (2) reduce to the NLS equation. In this special case the variational equations have the explicit solution

$$\alpha = \frac{a^2}{q}, \quad w = \beta = \frac{q^{1/2}}{2^{1/2}a}, \quad \sigma = a^2 - \frac{k^2}{2}, \tag{18}$$

which is the exact NLS soliton.

B. Uniform nematicon theory for the line bore

Once an approximate solution for the nematicon in 1+1 dimensions has been found, it can be used to find an approximation to the undular bore generated from a shock using the method of Grimshaw and Smyth [24]. This method is based on assuming that the shock is resolved by diffraction into a train of uniform nematicons. The profile amplitude and spacing are calculated by using global conservation laws [24], which must hold no matter what form of solution is used. Of course, this uniform nematicon approximation cannot hold throughout the bore as its constituent waves must approach linear waves at its trailing edge. The uniform nematicon approximation is then valid near the front of the bore, where the waves are well approximated by nematicons. The mass and energy conservation laws of the nematicon equations (2) in 1+1 dimensions are

$$i\frac{\partial}{\partial z}(|E|^2) + \frac{1}{2}\frac{\partial}{\partial x}(E^*E_x - EE_x^*) = 0, \tag{19}$$

$$i\frac{\partial}{\partial z}(|E_x|^2 - 4\theta|E|^2 + \nu\theta_x^2 + 2q\theta^2) + \frac{1}{2}\frac{\partial}{\partial x} \times (E_x^*E_{xx} - E_xE_{xx}^* - 4\theta E^*E_x + 4\theta EE_x^* - 4i\nu\theta_x\theta_z) = 0, \tag{20}$$

respectively. It should be noted that these conservation laws are named from invariances of the Lagrangian (9) [34] but do not correspond to the same quantities in optics. For instance, the mass conservation law (19) corresponds to conservation of power in optics.

To find an approximate solution for the bore we assume that at z there are N nematicons of uniform amplitude generated from the shock. The conserved quantities are then N times those for a single nematicon. On integrating the conservation laws from $x=-\infty$ to $x=\infty$, contributions from the flux terms (x derivative terms) are picked up at $x=-\infty$ due to the condition (3) holding at $x=-\infty$. There is no flux contribution from $x=\infty$ as the condition (3) gives that $E=\theta=0$ at $x=\infty$. Integrating the conservation equations then gives

$$\frac{d}{dz}\int_{-\infty}^{\infty}|E|^2dx = ka_m^2, \tag{21}$$

$$\frac{d}{dz}\int_{-\infty}^{\infty}(|E_x|^2 - 4\theta|E|^2 + \nu\theta_x^2 + 2q\theta^2)dx = ka_m^2\left(k^2 - 4\frac{a_m^2}{q}\right). \tag{22}$$

Since we are assuming that N identical nematicons have been generated, the integrals on the left hand side of Eq. (22) are N times the integral for one nematicon. From the trial functions (10) the mass and energy for a single nematicon can be evaluated as

$$\int_{-\infty}^{\infty}|E|^2dx = 2a^2w,$$

$$\int_{-\infty}^{\infty}(|E_x|^2 - 4\theta|E|^2 + \nu\theta_x^2 + 2q\theta^2)dx = \left(\frac{2a^2}{3w} + \frac{16\nu\alpha^2}{15\beta} + 2k^2a^2w + \frac{8}{3}q\alpha^2\beta - \alpha a^2 I\right). \tag{23}$$

The conservation relations (21) and (22) then provide

$$2a^2wN_z = ka_m^2,$$

$$\left(\frac{2a^2}{3w} + \frac{16\nu\alpha^2}{15\beta} + 2k^2a^2w + \frac{8}{3}q\alpha^2\beta - \alpha a^2 I\right)N_z = ka_m^2\left(k^2 - 4\frac{a_m^2}{q}\right). \tag{24}$$

Eliminating N_z gives the transcendental equation

$$\frac{2a^2}{3w} + \frac{16\nu\alpha^2}{15\beta} + \frac{8}{3}q\alpha^2\beta - \alpha a^2 I = -\frac{8a_m^2}{q}a^2w, \tag{25}$$

which determines the profile amplitude a on using Eqs. (15)–(17).

For a certain profile amplitude a_m of the initial jump and given q and ν Eqs. (15)–(17) and (25) are four equations for the four parameters of the nematicons generated from the shock.

For $\nu=0$ the uniform nematicon theory has the exact analytical solution with

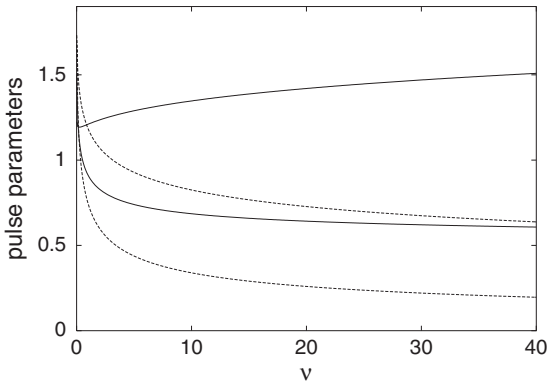

FIG. 1. Variation of nematicon bore parameters vs ν. Shown are a (upper solid line), α (lower solid line), w^{-1} (upper dashed line), β^{-1} (lower dashed line) from uniform soliton theory. The other parameters are $a_m=0.5$ and $q=1$.

$$a=\sqrt{6}a_m, \quad \alpha=\frac{6a_m^2}{q}, \quad w=\beta=\frac{\sqrt{q}}{2\sqrt{3}a_m}. \tag{26}$$

Hence, in this limit, the lead nematicon has an electric field amplitude which is 2.45 times the height of the initial jump (shock) and the optic axis distribution has an amplitude of 6 times the initial jump (in θ). By way of contrast, for the KdV undular bore the lead soliton is twice the height of the initial jump.

Figure 1 shows the predictions of uniform nematicon theory. a, α, w^{-1}, and β^{-1} are shown vs ν as given by Eqs. (15)–(17) and (25). The initial shock has a profile amplitude $a_m=0.5$ with $q=1$. At $\nu=0$ the nematicon has an electric field amplitude of $a=1.22$, while the optic axis distribution perturbation has amplitude $\alpha=1.5$. As ν increases the profile amplitude a, after a slight dip, increases as well, while the optic axis perturbation amplitude decreases. At $\nu=0$ the width of both distributions is $\beta=w=0.57$. As ν increases the widths of both profiles increase, with β, the width of the optical disturbance, becoming much larger than the width of the electric field profile w. This is consistent with the nonlocal limit, as for $\nu\to\infty$ the director distribution becomes much broader than the electric field.

IV. COMPARISON WITH NUMERICAL SOLUTIONS

In this section numerical solutions of the nematicon equations (2) are compared with the semianalytical solutions developed for line bores. The numerical solutions were found using the Dufort-Frankel finite difference scheme to solve the electric field equation, the first of Eqs. (2). For the director equation, the second of Eqs. (2), Gauss-Seidel iteration was used with successive over relaxation. An advantage of the Dufort-Frankel and Gauss-Seidel schemes is that they are both explicit methods with low storage costs. The step sizes used were $\Delta x=0.4$ and $\Delta z=4\times10^{-3}$. Note that $\Delta z/\Delta x$ must be small to ensure consistency of the DuFort-Frankel finite difference scheme.

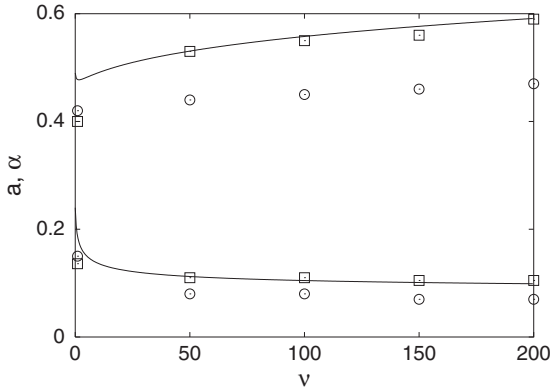

FIG. 2. Profile amplitudes vs ν. Shown is a, α (solid lines) from uniform soliton theory. Numerical estimates are for the first nematicon (circles) and the average maximum amplitude (squares). The other parameters are $a_m=0.2$, $q=1$, and $k=0$.

A. The line bore

Figure 2 displays the profile and optical axis distribution amplitudes, a and α, vs ν. The other parameters are $a_m=0.2$, $q=1$, and $k=1$. Shown are the prediction of uniform soliton theory and the numerical solutions. Two different numerical estimates of the profile amplitudes are visible. One estimate is the amplitude of the first nematicon generated by the shock (initial jump) at the z value for which the nematicon has fully formed. The second estimate is the maximum profile amplitude in the bore averaged from the z position at which the first nematicon has formed until the z value at which modulational instability dominates. An averaging process is needed as there is some oscillation in the profile amplitude while the bore develops.

For small ν the undular bore is qualitatively similar to that for the KdV equation (see Fig. 3), while for large ν the nematicons which are generated interact with each other nonlocally due to the broad response of the nematics causing a wide potential well enclosing all the solitons in the bore (see Fig. 4). Hence for small ν the profile amplitude does not vary much once it is fully formed, while for large ν the maximum profile amplitude varies with z since the waves interact.

The general trend is that, as ν increases, the profile amplitude increases and that of the optic axis distribution de-

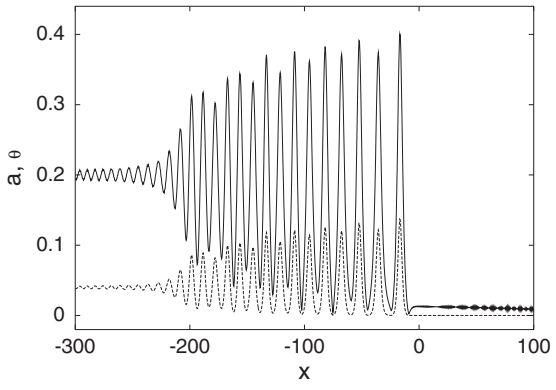

FIG. 3. Numerical solutions of Eq. (2) vs x at $z=300$. Shown are $|E|$ (solid line) and θ (dashed line). The other parameters are $\nu=1$, $a_m=0.2$, $q=1$, and $k=0$.

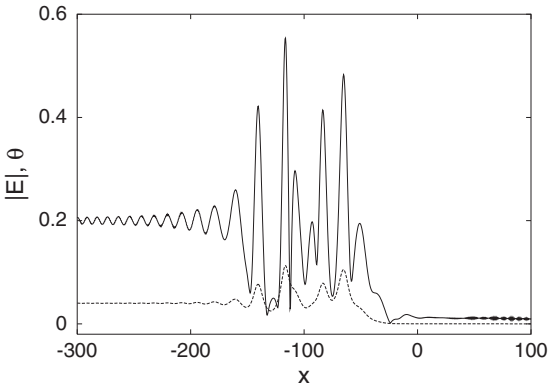

FIG. 4. Numerical solutions of Eq. (2) vs x at $z=400$. Shown are $|E|$ (solid line) and θ (dashed line). The other parameters are $\nu=50$, $a_m=0.2$, $q=1$, and $k=0$.

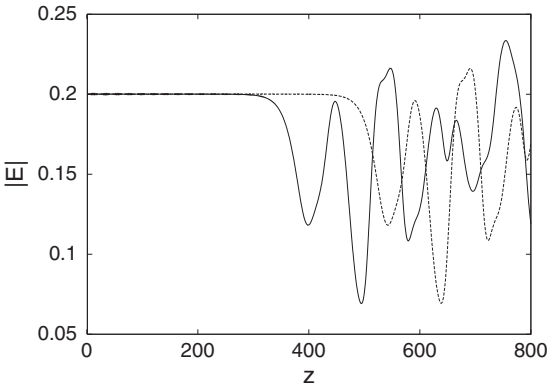

FIG. 5. Numerical solutions of nematicon equations (2) vs z. Shown are $|E|$ vs z for $\epsilon_1=10^{-6}$ (solid line) and $\epsilon_1=10^{-8}$ (dashed line). The other parameters are $\nu=50$, $a_m=0.2$, $q=1$, $k=0$, and $\mu=0.15$.

creases. The comparison between the theoretical results and the numerical estimates of the maximum nematicon amplitude is excellent. For the first nematicon of the bore the uniform soliton theory overestimates the numerical predictions by about 25%.

Figure 3 shows the numerical solutions for $|E|$ and θ vs x at $z=300$. The other parameters are $\nu=1$, $a_m=0.2$, $q=1$, and $k=0$. This figure shows a classical undular bore with nematicons at the front of the bore and linear waves of small amplitude at the rear of the bore. The lead wave has amplitude $a=0.4$ and $\alpha=0.14$. The uniform nematicon approximation of the present work gives $a=0.48$ and $\alpha=0.18$, which overestimate the numerical values by 20% and 28%, respectively. As this example is for the local limit the optical axis distribution has approximately the same width as the electric field. Also, the lead wave in the bore is stationary. This is in accord with the prediction $V=k=0$ of the current uniform nematicon approximation. A numerical solution for the same parameter values, except with $k=1$, yields an identical bore which is shifted to the right by $x=293$. This corresponds to a numerical propagation constant $V=0.97$, which is very close to the theoretical prediction $V=k=1$. It should be noted that for this example MI does not occur until $z=600$.

Figure 4 shows the numerical solution of the nematicon equations (2) for $|E|$ and θ vs x at $z=400$. The other parameters are $\nu=50$, $a_m=0.2$, $q=1$, and $k=0$. A classical bore, as seen in Fig. 3, has a structure where the waves decrease in amplitude from the front to the rear. In this nonlocal case this pattern disappears with the waves no longer ordered by amplitude. Also it can be seen from the figure that there are less director peaks in the bore than electric field peaks. The large nonlocality ($\nu=50$) of this example has resulted in a broad director response, which wipes out many individual peaks. Moreover, the director profiles are now broader than the electric field profiles ($\beta=6.9>w=2.9$), as expected, and hence the nematicons interact with each other through this broad potential well, as discussed above. The amplitude of the highest nematicon varies in a complicated manner with z due to this interaction. However, the average maximum amplitude, calculated from $z=100$ when the first nematicon has fully formed, to $z=1200$, after which modulational instability dominates, is $a=0.55$ and $\alpha=0.11$. This is very close to the estimates from uniform soliton theory of $a=0.53$ and $\alpha=0.11$. Again the bore is stationary, as $k=0$. For $k=1$ the numerical propagation constant is $V=1.03$, which is very close to the theoretical result $V=k=1$.

To investigate the onset of MI for the collisionless shock considered here we add a small perturbation to the cw boundary condition (3) of the form

$$\epsilon = \epsilon_1 \cos(\mu x). \tag{27}$$

Figure 5 shows the numerical solution of the nematicon equations, $|E|$ vs z, at an x location well behind the developing bore. The other parameter values are $\nu=50$, $a_m=0.2$, $q=1$, $k=0$, and $\mu=0.15$. For these parameter values the instability band (8) is (0, 0.30), so the choice $\mu=0.15$ lies in the center of the instability band. When $\epsilon_1=10^{-6}$ the figure shows that the onset of MI occurs at $z\approx400$, with large amplitude oscillations occurring for larger z. For $\epsilon_1=10^{-8}$ the onset of MI is delayed to $z\approx550$, with a similar oscillatory pattern occurring for larger z. The onset of MI can be theoretically predicted from the stability analysis in Sec. II B. From Eq. (7) the growth rate of the perturbation, or the gain, for the examples considered here is $\lambda=0.032$. We set $\epsilon_1 e^{\lambda z}=O(0.1)$, which is the order of magnitude of the first oscillation generated by the MI. Assuming $\epsilon_1=10^{-y}$ gives the linear relation $z=72(y-1)$, which estimates the onset of MI as a function of the magnitude of the initial perturbation. For the examples of Fig. 5 we obtain $z=360$ and $z=505$ ($y=6$ and 8, respectively) as theoretical estimates for the location of the onset of MI. It can be seen that these theoretical estimates are very good as they vary by less than 10% from the numerical values. In the case where MI is generated by computer round-off error $\epsilon_1\approx10^{-16}$ as FORTRAN double precision code was used to generate the numerical solutions. In this case the theoretical estimate for the onset of MI is $z=72(16-1)=1080$, which again has a 10% variation from the numerical onset at $z\approx1200$.

Figure 6 shows the numerical solution of the nematicon equations, $|E|$ vs z, at an x location well behind the developing bore for various values of ν, with $a_m=0.2$, $q=1$, $k=0$, and $\epsilon_1=10^{-6}$. For $\nu=50$ the instability band (8) is (0, 0.30),

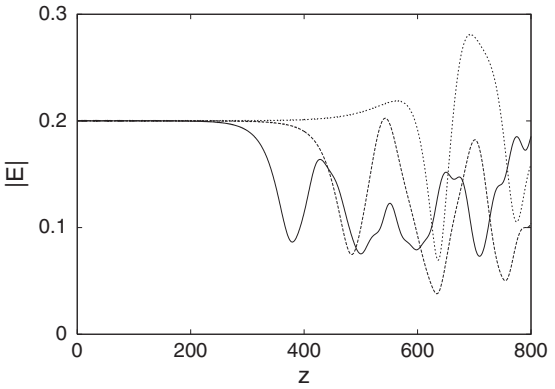

FIG. 6. Numerical solution of nematicon equations (2) vs z. Shown are $|E|$ vs z for $\nu=50$ (solid line), $\nu=100$ (long dashes), and $\nu=200$ (short dashes). The other parameter values are $a_m=0.2$, $q=1$, $k=0$, and $\epsilon_1=10^{-6}$.

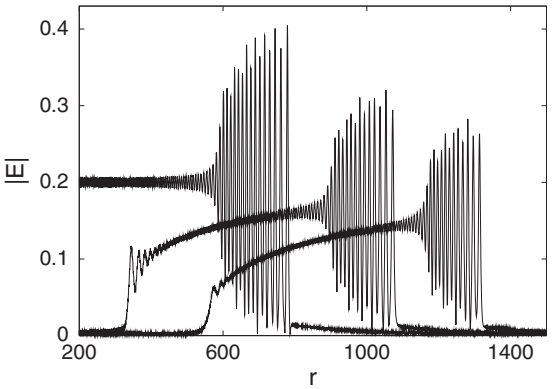

FIG. 7. Numerical solutions of nematicon equations (2) vs r at $z=300$. Shown are $|E|$ for $k=0$ (the left bore), $k=1$ (the middle bore), and $k=2$ (the right bore). The other parameters are $\nu=1$, $a_m=0.2$, $q=1$, and $r_0=800$.

with the maximum gain $\lambda_1(\mu=0.2)=0.0346$. For $\nu=100$ we have a maximum gain $\lambda_2(\mu=0.18)=0.0270$ and for $\nu=200$ the maximum gain is $\lambda_3(\mu=0.15)=0.0207$. The numerical solutions shown in Fig. 6 use the perturbation (27) with μ values corresponding to the maximum gain. The figure illustrates that the onset of MI is suppressed by increased nonlocality, as it occurs for larger z as ν increases. The onset of MI occurs at $z=380$, 484, and 636 for the three examples $\nu=50$, 100, and 200, respectively.

Again a simple relation, which for these parameter choices is $z=11.51/\lambda$, can be derived to predict the onset of MI. Hence the three theoretical estimates for the onset of MI are $z=333$, 426, and 556, respectively. These predictions underestimate the actual onset of MI slightly, by about 12%.

From a practical viewpoint the z location at which MI occurs in typical experimental scenarios is of great interest, as it determines whether or not the collisionless bores studied in this work can be experimentally observed. Reference [11] considered the experimental development of MI in nematic liquid crystals. In their Fig. 3 they showed that MI develops at $z\approx 300$ μm for an input beam with power $P=352$ mW. This power level is very high for experiments involving nematicons, however, with a power level of $P=O(10)$ mW much more typical, see [4,5,15]. The reason that such a high power level was used in this experimental work was that MI was not observable over typical experimental length scales using lower power levels. Expression (5) in [11] gives the MI gain $\lambda \propto P^{1/2}$, which implies that the onset of MI will occur at $z\approx(352/17)^{1/2}300=1.26$ mm for a power $P=17$ mW. [35] showed that $Z=500$ is a typical nondimensional cell length, corresponding to experimental cells with dimensional lengths of 1–2 mm, so for many typical experimental scenarios involving nematic liquid crystals collisionless shocks will develop on length scales shorter than MI does.

B. The circular bore

Let us consider the 2+1 dimensional nematicon equations with circular symmetry, i.e., $E=E(r,z)$ and $\theta=\theta(r,z)$, where $r=\sqrt{x^2+y^2}$. The appropriate boundary condition is then

$$E=\begin{cases} a_m e^{i(kr-\omega z)}, & 0<r<r_0, \\ 0, & r>r_0, \end{cases}$$

$$\theta=\begin{cases} \dfrac{a_m^2}{q}, & 0<r<r_0, \\ 0, & r>r_0 \end{cases} \tag{28}$$

at $z=0$, where the expression for ω is given in Eq. (4). The cw wave, which forms the boundary condition for $r<r_0$, is the 1+1 dimensional cw solution (2). In contrast to the 1+1 dimensional case, however, the cw is only an exact solution of the 2+1 dimensional governing equations for a stationary bore, for which $k=0$. For $k>0$ the cw in Eq. (28) is only a valid approximation for $r\gg 1$ and hence will evolve in z, especially near the origin $r=0$.

Figure 7 shows the numerical solution of the 2+1 dimensional nematicon equations (2), $|E|$ vs r at $z=300$. The other parameters are $\nu=1$, $a_m=0.2$, $q=1$, and $r_0=800$. For $k=0$ a stationary cw exists and the circular bore is qualitatively similar to the corresponding line bore of Fig. 3. Note that $|E|\to a_m$ as $r\to 0$ for the stationary circular bore, as the cw is an exact solution of the governing equations. The lead wave of the circular bore has $a=0.4$ and $\alpha=0.14$, which are identical results to those for the corresponding line bore of Fig. 3.

For nonzero k the circular bore is quite different to the stationary case as it propagates outwards with a central dark zone forming, in which the electric field intensity is low. Qualitatively this is similar to experimental results for the formation of a circular bore in a defocusing medium [21,22] (see Fig. 5 of [21] and Figs. 2 and 6 of [22]). For $k=1$ the lead wave has $a=0.32$ and $\alpha=0.09$ at $r=1050$, while for $k=2$ the lead wave has $a=0.28$ and $\alpha=0.07$ at $r=1310$. These locations correspond to numerical values of $V=0.97$ and $V=1.8$, respectively. For the line bore it can be shown analytically that $V=k$, so the numerical propagation constants for the circular bore are slightly lower than the theoretical value in 1+1 dimensions.

As r increases it can be seen that the amplitude of the nematicons in the expanding circular bores decrease. This is due to geometric spreading. A simple geometric optics analy-

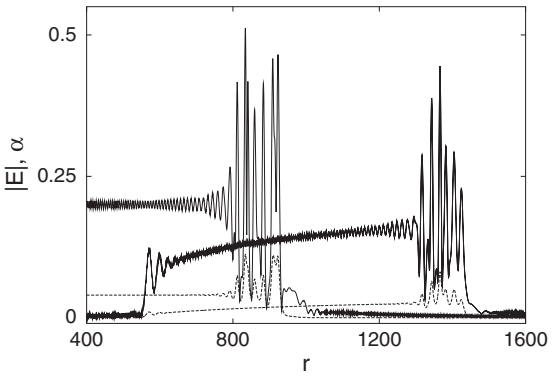

FIG. 8. Numerical solutions of the nematicon equations (2) vs r at $z=500$. Shown are $|E|$ (solid lines) and α (dashed lines) for $k=0$ (the left bore) and $k=1$ (the right bore). The other parameters are $\nu=50$, $a_m=0.2$, $q=1$, and $r_0=1000$.

sis shows that the profile amplitude decreases like $a\sim r^{-1/2}$ for large r, while the director response decreases like $\alpha\sim r^{-1}$, again for large r. Using this geometric optics analysis and numerical results for the circular stationary bore gives a prediction for the amplitude of the largest wave in the bore of $a=(780/1050)^{1/2}0.40=0.34$ and $\alpha=(780/1050)0.14=0.10$ for the $k=1$ case. For $k=2$ geometric optics gives predictions of $a=0.31$ and $\alpha=0.08$. These results are very close to the actual numerical amplitudes of the expanding bores with the geometric optics explaining about 75% of the decay in the profile amplitude and over 90% of the decay in the director response.

Figure 8 shows the numerical solution of the 2+1 dimensional nematicon equations (2), $|E|$ and θ vs r, at $z=500$. The other parameters are $\nu=1$, $a_m=0.2$, $q=1$, and $r_0=1000$. For $k=0$ the circular bore is stationary and is qualitatively similar to the corresponding line bore of Fig. 4. As for the line bore case the large nonlocality causes the nematicons to interact via the broad director response. For the stationary circular bore the largest nematicon has $a=0.51$ and $\alpha=0.11$, while the leading edge of the bore is at $r=930$. For $k=1$ the bore propagates outwards. The leading edge of the bore is now at $r=1440$. The amplitudes of the largest nematicon in this expanding bore are $a=0.45$ and $\alpha=0.08$. For this expanding bore $V=1.02$, very close to the 1+1 dimensional estimate of 1.

In the discussion of Fig. 4, which dealt with a line bore, it was explained how nonlocality causes the maximum profile amplitude in a bore to vary in a complicated manner with z since the nematicons are interacting via the director. It was found, however, that the average of the maximum amplitudes, over the length of the cell, compared well with the predictions from uniform nematicon theory. For an expanding circular bore, however, the predictions of uniform nematicon theory must be modified using geometric optics to allow for the effect of geometric spreading.

For an expanding circular bore the z-weighted averages of the electric field and director responses in a domain extending from $z=0$ to $z=z_1$ are

$$\frac{a}{z_1}\int_0^{z_1}\frac{dz}{[1+(Vz/r_0)]^{1/2}}=\frac{2a}{Vz_1}[(r_0^2+Vr_0z_1)^{1/2}-r_0],$$

$$\frac{\alpha}{z_1}\int_0^{z_1}\frac{dz}{[1+(Vz/r_0)]}=\frac{r_0}{Vz_1}[\ln(r_0+Vz_1)-\ln(r_0)]. \quad (29)$$

The predictions of uniform nematicon theory for the line bore are $a=0.54$ and $\alpha=0.11$ for the parameters of Fig. 8. For the stationary circular bore, for $z_1=1200$, the average maximum amplitudes are $a=0.55$ and $\alpha=0.12$, nearly identical to the line bore results.

For the expanding circular bore the predictions of uniform nematicon theory must be combined with Eq. (29), which gives predictions of $a=0.44$ and $\alpha=0.07$ using $z_1=1200$, $V=1$, and the other relevant parameters of Fig. 8. The numerical averages for this expanding bore are found to be $a=0.40$ and $\alpha=0.07$, which again gives an excellent comparison with the theoretical predictions.

In summary, it was found that the analytical theory developed for the line bore geometry also works well for circular bores of large initial radius, giving accurate predictions. Uniform nematicon theory can be used directly for a stationary circular bore, but must be combined with a geometric optics analysis for an expanding circular bore.

V. CONCLUSIONS

The evolution of collisionless shocks in a nonlocal, focusing medium, namely a nematic liquid crystal, was considered both analytically and numerically. The resolution of an initial discontinuity, or optical shock, was examined for both the 1+1 dimensional nematicon equations (a line bore) and the 2+1 dimensional nematicon equations with circular symmetry (a circular bore).

A semianalytical solution, which predicts the amplitudes of the largest waves in the bores, was derived from uniform nematicon theory, which in turn was developed from conservation laws and the assumption that a train of uniform nematicons is generated by the shock. The semianalytical predictions were found to be in excellent agreement with numerical solutions for both line and circular bores. The present semianalytical theory represents a suitable method of finding analytical bore solutions for a focusing medium.

Due to solutions of the focusing equations being subject to modulational instability, the boundary value problems considered here are, in fact, ill posed. However, it was shown that collisionless shocks should develop on experimentally observable length scales, shorter than for MI.

This study motivates and will encourage experimental observations of collisionless shocks in nematic liquid crystals and other nonlocal media.

Last, the uniform nematicon theory is expected to be useful for predicting the generation of dark nematicons in the defocusing version of the present nematicon equations, applicable to thermal media. This is a topic of currently ongoing research.

ACKNOWLEDGMENT

This research was supported by the Engineering and Physical Sciences Research Council (EPSRC) under Grant No. EP/C548612/1.

[1] Y. S. Kivshar and G. P. Agrawal, *Optical Solitons. From Fibers to Photonic Crystals* (Academic, San Diego, 2003).
[2] I. C. Khoo, *Liquid Crystals: Physical Properties and Nonlinear Optical Phenomena* (Wiley, New York, 1995).
[3] G. Assanto, M. Peccianti, and C. Conti, Opt. Photonics News **14**, 44 (2003).
[4] G. Assanto and M. Peccianti, IEEE J. Quantum Electron. **39**, 13 (2003).
[5] C. Conti, M. Peccianti, and G. Assanto, Phys. Rev. Lett. **92**, 113902 (2004).
[6] G. Assanto, M. Peccianti, K. A. Brzdakiewicz, A. de Luca, and C. Umeton, J. Nonlinear Opt. Phys. Mater. **12**, 123 (2003).
[7] C. Conti, M. Peccianti, and G. Assanto, Phys. Rev. Lett. **91**, 073901 (2003).
[8] C. García-Reimbert, A. A. Minzoni, and N. F. Smyth, J. Opt. Soc. Am. B **23**, 294 (2006).
[9] C. García-Reimbert, A. A. Minzoni, N. F. Smyth, and A. L. Worthy, J. Opt. Soc. Am. B **23**, 2551 (2006).
[10] A. A. Minzoni, N. F. Smyth, and A. L. Worthy, J. Opt. Soc. Am. B **24**, 1549 (2007).
[11] M. Peccianti, C. Conti, and G. Assanto, Phys. Rev. E **68**, 025602(R) (2003).
[12] G. Assanto, M. Peccianti, and C. Conti, IEEE J. Sel. Top. Quantum Electron. **10**, 862 (2003).
[13] M. Peccianti, C. Conti, E. Alberici, and G. Assanto, Laser Phys. Lett. **2**, 25 (2005).
[14] M. Peccianti and G. Assanto, Opt. Lett. **30**, 2290 (2005).
[15] M. Peccianti, C. Conti, G. Assanto, A. De Luca, and C. Umeton, Nature (London) **432**, 733 (2004).
[16] C. Conti, M. Peccianti, and G. Assanto, Phys. Rev. E **72**, 066614 (2005).
[17] G. P. Agrawal and C. Headley, Phys. Rev. A **46**, 1573 (1992).
[18] Y. S. Kivshar and B. A. Malomed, Opt. Lett. **18**, 485 (1993).
[19] W. Krolikowski, O. Bang, J. J. Rasmussen, and J. Wyller, Phys. Rev. E **64**, 016612 (2001).
[20] Y. Y. Lin, R.-K. Lee, and Y. S. Kivshar, J. Opt. Soc. Am. B **25**, 576 (2008).
[21] N. Ghofraniha, C. Conti, G. Ruocco, and S. Trillo, Phys. Rev. Lett. **99**, 043903 (2007).
[22] W. Wan, S. Jia, and Y. S. Fleischer, Nat. Phys. **3**, 46 (2007).
[23] G. B. Whitham, *Linear and Nonlinear Waves* (Wiley, New York, 1974).
[24] R. H. J. Grimshaw and N. F. Smyth, J. Fluid Mech. **169**, 429 (1986).
[25] N. F. Smyth, Proc. R. Soc. London, Ser. A **409**, 79 (1987).
[26] T. R. Marchant, Wave Motion **45**, 540 (2008).
[27] T. R. Marchant and N. F. Smyth, IMA J. Appl. Math. **70**, 796 (2005).
[28] M. Peccianti, A. Fratalocchi, and G. Assanto, Opt. Express **12**, 6524 (2004).
[29] P. D. Rasmussen, O. Bang, and W. Krolikowski, Phys. Rev. E **72**, 066611 (2005).
[30] C. García-Reimbert, G. Hume, A. A. Minzoni, and N. F. Smyth, Physica D **167**, 136 (2002).
[31] A. V. Gurevich and L. P. Pitaevskii, Zh. Eksp. Teor. Fiz. **65**, 590 (1973) [Sov. Phys. JETP **33**, 291 (1974)].
[32] T. R. Marchant and N. F. Smyth, Proc. R. Soc. London, Ser. A **458**, 857 (2002).
[33] T. R. Marchant and N. F. Smyth, IMA J. Appl. Math. **47**, 247 (1991).
[34] C. J. Kaup and A. C. Newell, Proc. R. Soc. London, Ser. A **361**, 413 (1978).
[35] T. R. Marchant and N. F. Smyth, J. Phys. A **41**, 365201 (2008).